

DYNAMIC RESPONSE OF A PULSED BURKE-SCHUMANN DIFFUSION FLAME

Jyh-Cherng Sheu
Dep. of Mech. Eng., The University of Iowa
Iowa City, Iowa 52242

Dennis P. Stocker
NASA Lewis Research Center
Cleveland, Ohio 44135

Lea-Der Chen
Dep. of Mech. Eng., The University of Iowa
Iowa City, Iowa 52242

Introduction

Turbulent flames are often envisioned as an ensemble of random vortices interacting with the combustion process. A better understanding of the vortex-flame interactions therefore would be useful in improving the modeling of turbulent diffusion flames. Substantial simplification may be made by investigating controlled interactions in a laminar flame, as opposed to random interactions in a turbulent flame [1]. The general goals of the research project are to improve our understanding of (A) the influence of buoyancy on co-flow diffusion flames, and (B) the effects of buoyancy on vortex-flame interactions in co-flow diffusion flames. As a first step toward Objective (B), we conducted a joint experimental and numerical investigation of the vortex-flame interaction. Vortices were produced by mechanically pulsing the fuel flow at a low frequency, e.g., 10 Hz.

Experiments were conducted using a non-flickering Burke-Schumann [2] flame in both microgravity (μg) and normal gravity (1g) as a means of varying the buoyant force without modification of the pressure (i.e., density). The effects of buoyant convection may then be determined by a comparison of the μg and 1g results. The μg results may also reveal the important mechanisms which are masked or overwhelmed by buoyant convection in 1g. A numerical investigation was conducted using a validated, time-accurate numerical code to study the underlying physics during the flame interaction and to assist the interpretation of the experimental results.

Numerical Model

The mathematical formulation was based on the Burke-Schumann flame sheet model [2]. The time-dependent, axisymmetric Navier-Stokes equations coupled with the continuity and mixture fraction equations were solved by a semi-implicit scheme, which was modified from that reported in [3], by application of a flux-corrected transport (FCT) term [4] to the QUICK-based convective flux and a second-order central differencing to the diffusional flux. The projection method was retained to solve the velocity and pressure coupling through a direct solver. Two computational grid distributions, 180 (axial) by 80 (radial) and 120 by 60, were employed to cover a computational domain of 20.1 cm (axial) by 2.33 cm (radial), matching the chimney of the experimental burner. The fuel jet diameter was set to 0.56 cm, matching the inner diameter of the experimental burner. The two different grid distributions predicted the same dynamical characteristics but the denser grid produced a better resolution for isotherm and vorticity images. Steady-state solutions were obtained for the non-pulsed case and used as the initial condition for the simulation. The computation was done using a computer Workstation (RISC-based CPU-50 MHz) or a Personal Computer (486-66 MHz, DX2). With the 120 by 60 grids, the CPU times for each time step (0.2 ms) are 5.1 s and 10.5 s for the Workstation and PC, respectively.

Modeling Results

The BSDF studied in this paper does not exhibit flickering in 1g (normal gravity) or 0g (zero gravity) for both the simulation and experimental results. In 0g, the predicted flame (stoichiometric boundary) is wider and slightly shorter than in 1g, in qualitative agreement with [5]; the luminous region of experimental μg diffusion flames were slightly taller than the 1g flames, however. To simulate the experimental pulsation of the fuel jet due to opening and closing of a solenoid valve, a sine-wave forcing with an amplitude of 80% of the mean fuel-jet velocity (u_j) was imposed on the fuel jet inlet boundary condition. The simulation shows that the imposed sine-wave perturbation results in periodic flame oscillation, responding to the imposed forcing and with a phase lag of between the maximum flame height and the maximum u_j during one forcing cycle. No tip cutting is seen at low velocity, e.g., $u_j = u_a$ (coflow air velocity) = 5 cm/s. The cutting occurs at higher velocities.

When the fuel-jet velocity is increased, flame-tip cutting (i.e., pinching and separation of the flame tip) is predicted for $u_j = u_a = 18$ cm/s, in both 0g and 1g, cf. Fig. 1. The flame contours at ten phase angles separated by 10 ms (or phase angle of 36 degrees) are shown. The 18 cm/s emulates the non-perturbed 20 cm/s condition in test 3 (cf., Table I). The arbitrarily chosen reference time, i.e., $t = 0$ ms, has a nearly matched flame shape at $t = 50$ ms for the 0g and 1g flames. The flame-tip cutting for the 1g flame occurs at $10 \text{ ms} < t < 20 \text{ ms}$, whereas in 0g, the flame tip detaches at $20 \text{ ms} < t < 30 \text{ ms}$. Unlike the 0g flame, the detached flame parcel in 1g disappeared within the 10 ms interval. The flame-tip cutting is a result of an enhanced local mixing which leads to a local mixture fraction below the stoichiometric value. This enhanced mixing can be attributed to the vortex-flame interaction in a 1g pulsed methane-air diffusion flame [6], in which the vortex was formed due to the buoyancy acceleration. The present simulation and experiments showed a similar tip-cutting in BSDF in μg . The predicted flow-field isotherm, vorticity, and velocity contours revealed a large vortex outside the flame in the BSDF with $u_j = u_a = 18$ cm/s for both the 0g and 1g conditions. The pulsation of the fuel jet was responsible for the formation of an initial vortex near the fuel nozzle. The tip cutting was seen to coincide with the formation of a new vortex near the flame tip in 1g, and below the instantaneous half flame-height in 0g.

Experiment

Tests in the 2.2-second Drop Tower at the NASA Lewis Research Center [7] were conducted by pulsing the fuel flow in a laminar BSDF. The nitrogen-diluted fuel (CH_4/N_2 50% by mole) was used to reduce the sooting since sooting obscures the true flame shape as determined from the video image. Dry air was the oxidizer, and all tests were performed at approximately 0.98 atm. The small cylindrical burner consisted of a glass chimney (i.d. of 4.66 cm and length of 20 cm) surrounding a thin-walled (0.04 cm) stainless-steel tube (i.d. of 0.56 cm), with a fuel-to-oxidizer tube diameter ratio of 0.12 [3]. Flow restrictions and straighteners were used to produce a flat velocity profile at the entrance of the annulus. The fuel tube had a straight length with a length-to-i.d. ratio of approximately 27, presumably having a parabolic flow at the exit. A single layer of fine wire mesh was placed across the outlet of the chimney to keep sand (the drop tower deceleration material) out of the burner.

The tests were performed with u_j in the range of 10 to 30 cm/s, measured with a mass flowmeter and without the pulsation. The fuel flow was pulsed at a low frequency in the range of 6.7 to 12.5 Hz by opening and closing a solenoid valve (specified response time of 5-10 ms) in the fuel supply line. The solenoid valve was closed for approximately 10 ms and then held open for the remainder of the cycle. Two particle filters (valve coefficient of 0.15) were positioned between the solenoid valve and the burner inlet to produce a small pressure drop, and thus limit the amplitude of the pulsating inlet velocity. The annular air velocity was nominally set to be equal to the non-perturbed fuel velocity. Regrettably, after cessation of these tests (due to a shutdown of the Drop Tower for rehabilitation) a noticeable leak in the oxidizer system between the flow meter and the burner was discovered. Even with the leak, the air velocity was such that the flame did not flicker when the fuel flow was not perturbed.

The flames were ignited in 1g prior to the drop, with a hot-wire ignitor which was retracted (about 1 cm) out of the flame following ignition. In a typical test, the flame was allowed to develop without pulsations for 2 s, and then pulsed for 3 s in 1g. After a pulsation-free period of 5 to 7 s, the flame was dropped and the pulsations were resumed (at 0.1 s into the drop) for 2 s in μg . Although 1g ignition leads to residual buoyant flows, the gas velocities were such that buoyant effects should be convected away in less than 1 s (e.g., a flame-zone velocity of 40 cm/s would convect buoyant effects from the 20-cm chimney in 0.5 s). Furthermore, the experiments of [8] showed that flames ignited in 1g will more quickly reach (nearly) steady conditions during the drop test, than

flames ignited in μg .

For the present investigation, the instrumentation was strictly photographic with a color video camera recording the flame's side view at 30 frames per second (or 60 fields per second) [3]. The flame response to the flow pulsations was quantified by a measurement of the flame height as a function of time, using an image-processing and object-tracking workstation at NASA Lewis [9]. When the tip cutting occurred, the detached flame parcel was included in the flame height determination [3].

Table I: Summary of Test Results.

Test	Test Conditions		Flame Response, ϕ , (and tip cutting)		Flame Height (cm)		
	Forcing Frequency (Hz)	Fuel Velocity (cm/s)			1g, without pulsations	Mean (and std. dev.) with pulsations	
			1g	μg		1g	μg
1	10	10	1 (n)	1 (n)	1.2	0.9 (0.1)	0.7 (0.1)
2	10	15	3 (n)	1 (n)	2.1	1.9 (1.1)	1.5 (0.2)
3	10	20	2 (y)	2 (n)	2.7	2.9 (2.0)	2.3 (0.7)
4	10	25	2 (y)	2 (y)	3.4	4.1 (2.6)	3.3 (1.3)
5	10	30	1 (y)	2 (y)	4.3	5.0 (2.1)	4.2 (1.8)
6	6.7	20	2 (n)	1 (n)	2.6	2.4 (1.5)	2.3 (0.8)
7	8.3	20	2 (n)	1 (n)	2.6	2.6 (1.7)	2.3 (0.6)
3	10.0	20	2 (y)	2 (n)	2.7	2.9 (2.0)	2.3 (0.7)
8	12.5	20	2 (y)	3 (y)	2.7	2.5 (1.8)	2.1 (1.0)

Experimental Results

The video recording showed that the flames pulsated in response to the flow perturbations, and tip cutting was sometimes observed. When the flow was pulsed, the flames appeared to be strongly flickering, although the oscillations were the result of the forced perturbations and not buoyancy-generated instabilities. In addition to the fundamental frequency (i.e., showing the perturbation frequency in the response), the flame also exhibited a subharmonic response which varied with the gravity level, frequency, and flow rate. The subharmonic flame response can be seen in the photographs reported in [3]. For example, when the fuel jet with a mean velocity of 18 cm/s and pulsed at 10 Hz (as in Fig. 1), the flame responded subharmonically at 5 Hz in both μg and 1g as shown by the flame-height plots in Fig. 2; the flame-tip cutting was observed in 1g but not in μg . In other tests, however, the flame responded differently in μg and in 1g. A summary of the test results is shown in Table I.

A flame frequency response parameter, ϕ , can be defined to be the ratio of (*number of fuel-flow-cycles imposed*) to (*number of flame-shape-oscillations in response*) to describe the dynamic characteristics. For example, ϕ is equal to 2 for both gravity levels shown in Fig. 2. As seen in Table I, the mean flame heights were slightly greater in 1g than μg , in contrary to the steady-state predictions of [10-12] or earlier observations of non-perturbed BSDF [5, 8, 10, 11] in which the μg flames were slightly taller than the 1g flames. However, the observation of the mean flame height being slightly less in μg is in agreement with the numerical predictions presented in this paper.

The flame height as a function of fuel flow is shown in Fig. 3. For both 1g and μg conditions, the mean flame height increased linearly proportional to the fuel flow rate (as measured when it was not perturbed). The perturbed flows were not measured; thus, the figures can be misleading because the mean perturbed flow is lower than the non-perturbed value. For this reason, the height of the non-perturbed 1g flame was included in the figures. In general, the flame-height oscillation amplitude increased with increasing flow rate, and the relative position of the mean height within the amplitude range appeared to be related to ϕ .

The variation in forcing frequency over the range of 6.7 to 12.5 Hz had a limited effect on the flame response in 1g. All four flames in Table I (i.e. with four different u_j values) responded bimodally (i.e., $\phi_{1g} = 2$), and since the fuel flow was approximately fixed, the flame height oscillations were also fairly similar in the observed maximum, mean, and minimum heights. The test procedure resulted in a reduction in fuel flow with increased frequency, because the flow rate was set under no perturbations and a constant valve closure time for each cycle

was used for all frequencies (i.e., 10 ms). The most significant effect of the forcing frequency was on the tip cutting, which was apparent in the video record for the high frequencies but not the low frequencies. However, it was also possible that the flame tip cut between video frames because the tip often pinched partially when cutting was not apparent. In μg , the flame response becomes increasingly subharmonic as the forcing frequency was increased. Other than the change in ϕ , the height oscillation of the μg flames was only moderately affected by the forcing frequency (with test 8 at $\phi_{\mu\text{g}} = 3$ showing the most dramatic change, cf. Table I). The flame frequency response, ϕ , generally increased with increasing fuel flow and forcing frequency in μg ; but ϕ varied non-monotonically with fuel flow and it was not affected by the forcing frequency in 1g. However, the tip cutting occurrence increased in both 1g and μg with increasing fuel flow or forcing frequency.

The predicted flame heights at different fuel-jet velocities are also shown in Fig. 3. The predicted mean flame height increased linearly with increasing u_j , similar to the trend observed in the experiments. The predicted mean flame heights were longer than the experimental data, but the discrepancy decreased as the fuel-jet velocity was increased. The predicted mean flame length regresses to zero at $u_j = 0$ while there is an offset for the experimental data. The offset is due to the perturbation technique which diminished the flow rate from that reported. The predictions also showed $\phi = 1$ for all the conditions examined; the experiments, however, had different ϕ values, cf. Table I.

Discussion

The flow characteristics during the tip cutting can be deduced from numerical visualization based on the predicted isotherms and vorticity. For example, in 0g and 1g flames, large vortical structures (or concentrated vorticities) were formed outside the stoichiometric surface. These concentrated vorticities were caused by the sharp velocity gradient adjacent to the injector wall, and first appeared near the fuel nozzle and were then convected downstream. In 0g, the vorticity strength decayed rapidly when the vortex was convected downstream, but this rapid decay was not observed in 1g. In 1g, the downstream maximum-vorticity was found to be comparable to (or even slightly higher than) the maximum at the fuel jet exit. Both the buoyancy acceleration and volumetric expansion significantly affected the species transport (i.e., the mixture fraction). For example, the 1g flame length continued to increase beyond the phase angle or the time instant of the maximum fuel-jet velocity at nozzle exit because of buoyant convection of the stoichiometric surface. The volumetric expansion, however, appeared to "hold up" the flame tip at certain phase angles during the forcing. In 0g, the predicted tip cutting was located at below half of the instantaneous flame height at a phase angle having a zero fuel-jet velocity at the nozzle exit. In 1g, the tip cutting occurred near the flame tip at a phase angle before the zero fuel-jet velocity was reached. The unsteady flow due to the pulsation of the fuel jet was responsible for the high vorticity value at the nozzle exit and responsible for the vortex-flame interaction. The buoyant acceleration in 1g enhances the downstream convection of combustion products, and the vortex growth. In 0g, the volumetric expansion in the fuel-lean region appeared to be a sink term in the vorticity budget; whereas in 1g, the buoyant acceleration was a source term in the fuel-lean region. The observation was consistent with theoretical analysis of the vorticity equation of a jet diffusion flame reported in [13].

The numerical simulation predicted the BSDF tip-cutting in response to the periodic forcing of the fuel jet. The simulation, however, did not predict the experimentally observed bimodal or trimodal response. On the other hand, the current numerical model was able to predict the subharmonic frequency (resulting from vortex merging) of the flame flicker for the condition reported in [14]. Thus, a parametric study was conducted to assess such effects on the flame response as different velocities, fuel-jet velocity (spatial) profile, driving waveform and driving frequency. Decreasing u_a to half or one-third of the fuel-jet velocity (i.e., to 9 or 6 cm/s) was used to simulate the leak in the experiments, but it yields only a slight decrease in flame length and the tip cutting was still predicted. The predicted ϕ value, however, did not change. Using a uniform or parabolic velocity profile at the fuel-nozzle exit did not change the prediction of ϕ either. A slightly longer maximum flame-height was predicted when the parabolic profile was used.

Three waveforms were used as the fuel-jet boundary condition in an effort to evaluate the effects due to the perturbed fuel-jet velocity profile since the profile was not quantified in the experiments. None of these waveforms, however, predicted a bimodal or trimodal response, nor a $\phi \neq 1$ response. The waveforms evaluated included (A) using a zero velocity for the initial 10 ms and followed by 20 cm/s for the remaining 90 ms of a 100 ms forcing cycle, (B) a zero velocity for the initial 10 ms, 32.5 cm/s for next 5 ms, and 19.27 cm/s for the remaining 85 ms, and (C) a zero velocity for the initial 10 ms, 53 cm/s at 10 ms and followed by an exponential

decay to preserve the averaged flow rate. The predicted flame length varied with these different waveforms; for example, the tip-cutting was not predicted. It was also observed that higher harmonic frequencies in the flow field were predicted with a 1-Hz or 2-Hz forcing of the fuel jet, when a higher-order scheme was used (i.e., the current FCT scheme). This higher harmonic frequency response, however, was not predicted when a lower-order scheme (e.g., an upwind) when the same grid resolution was used. Thus, a higher-order scheme is required for accurate prediction of dynamic response of the chemically reactive flow investigated in this paper.

To assess the effects due to the model assumptions on the prediction of flame response (or the failure in the prediction of the bimodal or trimodal response), the finite-rate chemistry, equal diffusion, and unity Lewis number assumptions were relaxed. The simulation based on the one-step global kinetics of Westbrook and Dryer [15], differential diffusion of different species, and with the non-unity Lewis number effect accounted for in the energy equation predicted essentially the same flame response, i.e., only with $\phi = 1$. The results suggested that the flame dynamics were dominated by convective flow, and the transport properties and finite rate chemistry played a secondary role. It should also be mentioned that the differential pressure across the solenoid valve was measured and there was no evidence to suggest that a sub-harmonic response existed in the valve opening and closing. Therefore, the failure to predict the bimodal or trimodal response was not due to the numerical model assumptions, nor was it due to the presence of a subharmonic response in valve characteristics. Further investigation is needed to resolve the discrepancy.

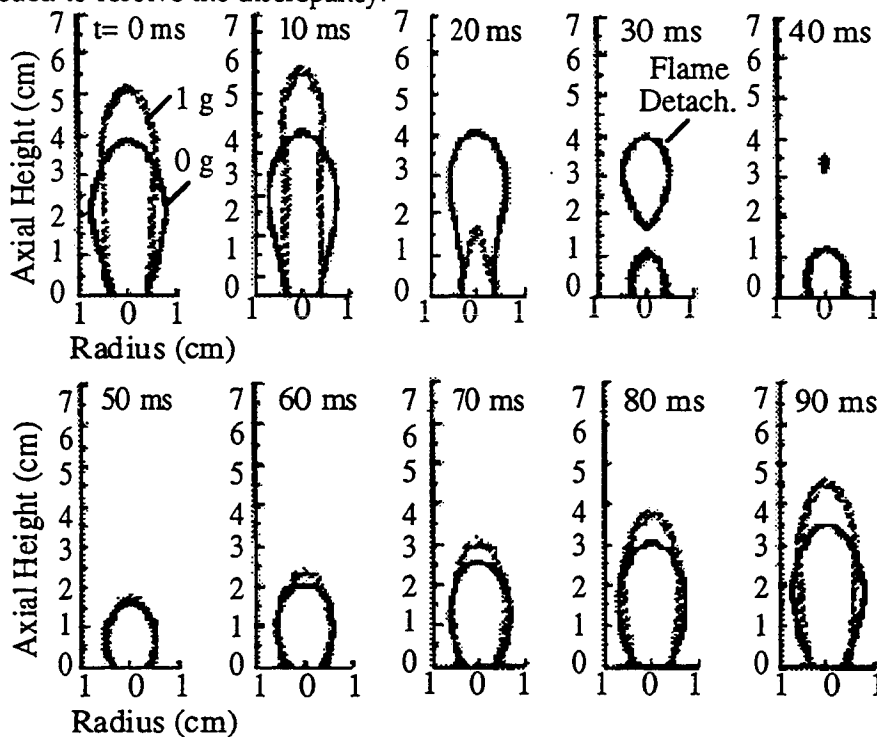


Figure 1. Predicted time evolution of flame shape with a 10-Hz driving (test 3, Table I).

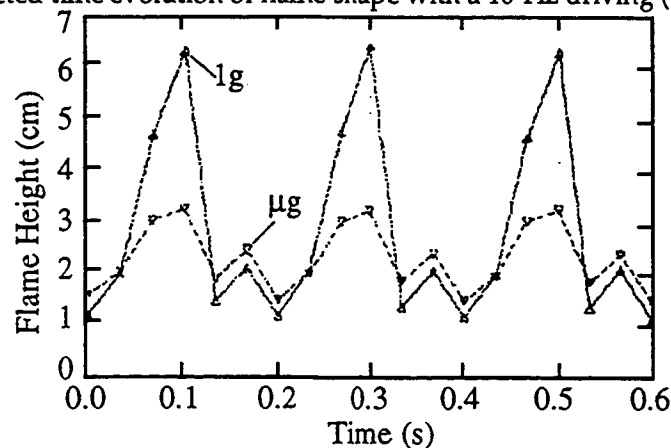


Figure 2. Observed flame height vs. time in 1g and μg with a 10-Hz driving (test 3, Table I).

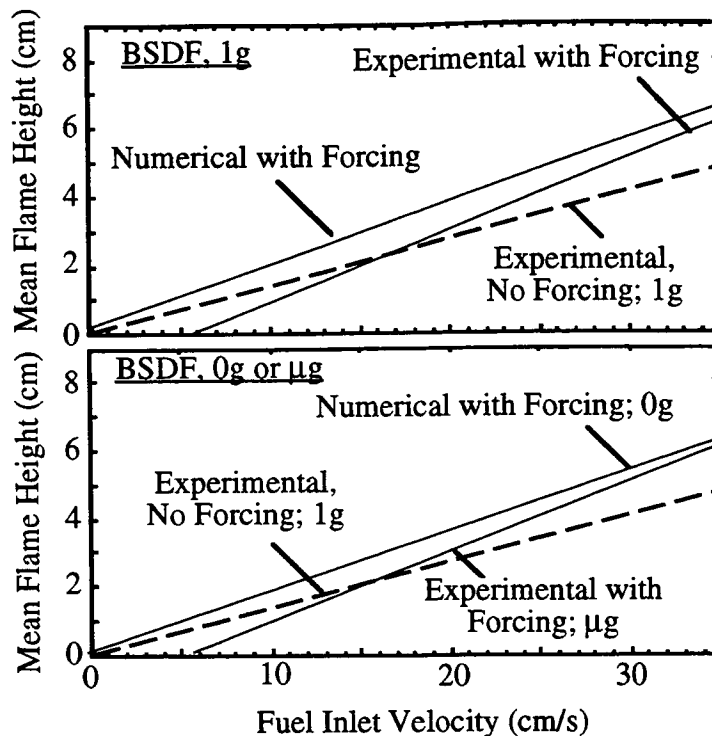


Figure 3. Flame height vs. non-perturbed fuel-jet inlet velocity; detached flame parcels are included and ϕ values are shown for fuel-jet inlet velocities of 5, 10, 20, 25 and 30 cm/s.

Acknowledgment

This research was supported by NASA Microgravity Science and Applications Division, Code UG, under Grant No. NAG3-1592.

References

1. Markstein, G.H. (1949). Third Symposium on Combustion, Flame and Explosion Phenomena Williams and Wilkins Co., Baltimore, Maryland, p. 162.
2. Burke, S.P., and Schumann, T.E.W. (1928). Ind and Engineer. Chem., Vol. 20, p. 998.
3. Stocker, D.P., Sheu, J.-C. and Chen, L.-D. (1993). Paper 93-065, 1993 Fall Meeting of the Western States Section, The Combustion Institute.
4. Zalesak S.T. (1979). J. of Comput. Phys., Vol. 31, p. 335.
5. Stocker, D.P. (1991). Paper No. 15 and No. 16, the 1991 Spring Technical Meeting of the Central States Section of The Combustion Institute, Nashville, Tennessee, April 22-24.
6. Strawa, A.W. and Cantwell, B.J. (1985). Phys. Fluids, Vol. 28, p. 2317.
7. Lekan, J. (1989). AIAA Paper No. 89-0236, (also appears as NASA TM-101397).
8. Stocker, D.P. (1990). Paper No. 42, the 1990 Spring Technical Meeting of the Central States Section of The Combustion Institute, Cincinnati, Ohio, May 20-22.
9. Klimek, R.B. and Paulick, M.J. (1992). Color Image Processing and Object Tracking Workstation. NASA TM 105561
10. Hegde, U. and Bahadori, M.Y. (1992). AIAA Paper No. 92-0334.
11. Hegde, U. and Bahadori, M.Y. (1992). An Analytical Model for Gravitational Effects on Burke-Schumann Flames. The 1992 Fall Western States Meeting of The Combustion Institute.
12. Hyer, P.V., Stocker, D.P., and Clark, I.O. (1993). AIAA Paper No. 93-0707.
13. Chen, L.-D., Roquemore, W.M., Goss, L.P., and Vilimpoc, V. (1991). Combust. Sci. Technol., Vol. 77, p. 41.
14. Chen, L.-D., Vilimpoc, V., Goss, L. P., Davis, R. W., Moore, E. F. and Roquemore, W. M. (1992). 24th Symp. (Internat.) on Combust., P. 303.
15. Westbrook, C.K. and Dryer, F.L. (1981). Combust. Sci. Technol., Vol. 27, p. 31.